Laboratory for Neutron Scattering and Imaging

Paul Scherrer Institut

HRPT - High Resolution Powder Diffractometer for Thermal Neutrons

Instrument responsibles: Vladimir Pomjakushin and Denis Sheptyakov

http://sinq.web.psi.ch/hrpt

Instrument layout and views at SINQ target station

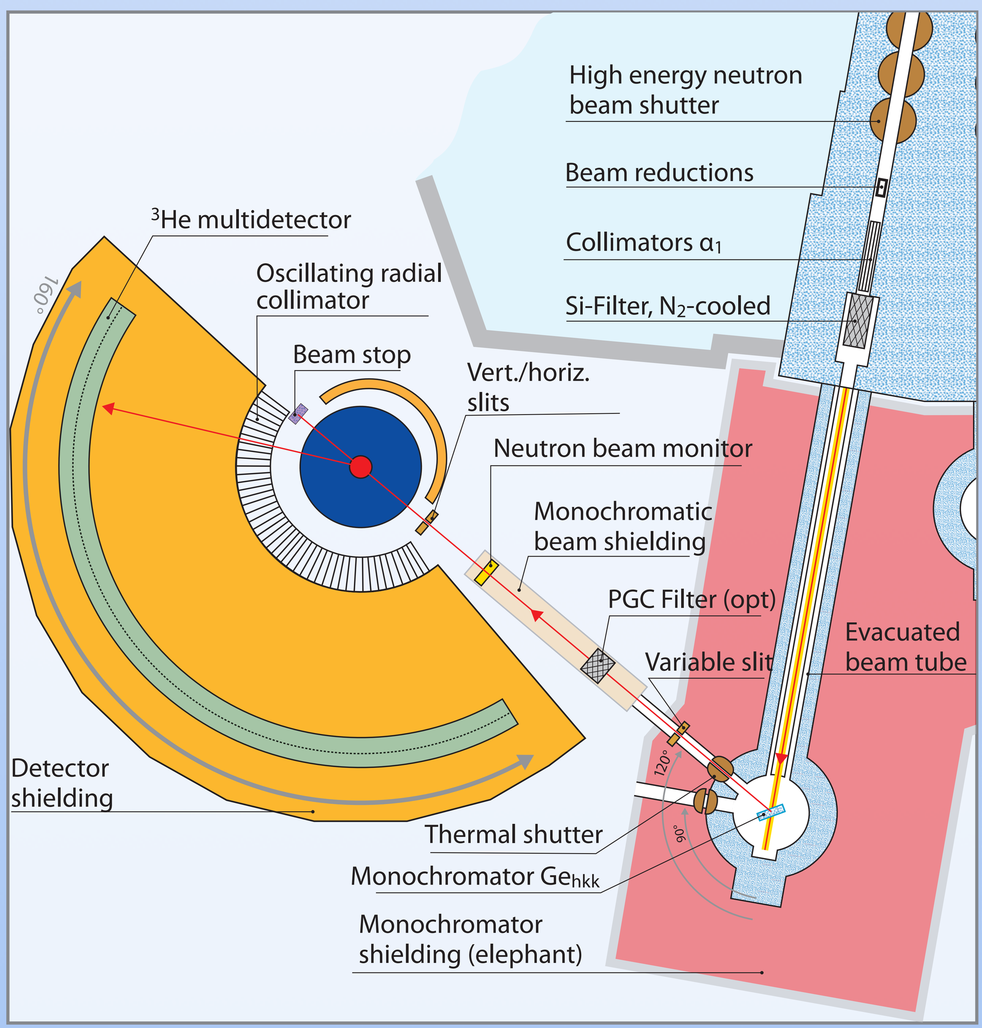

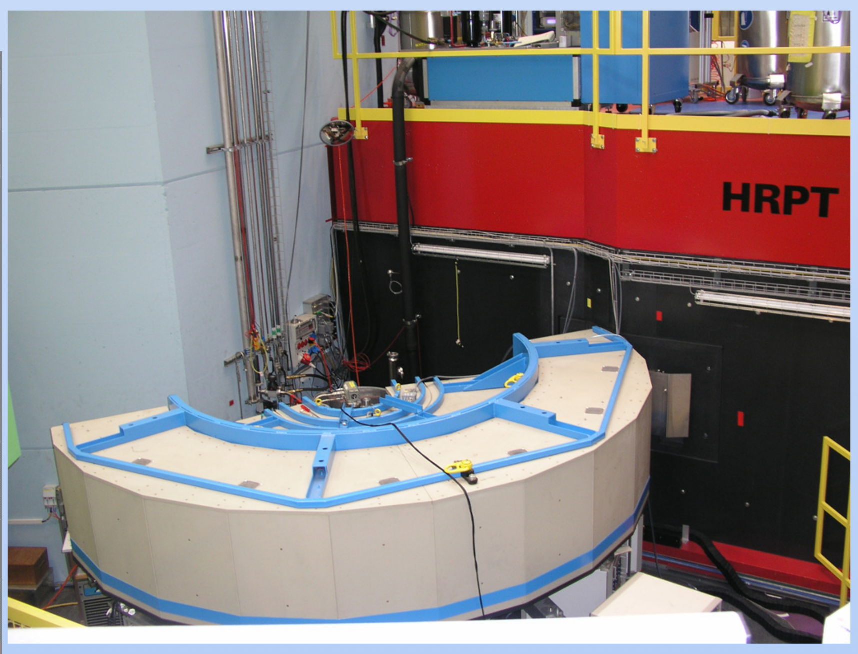

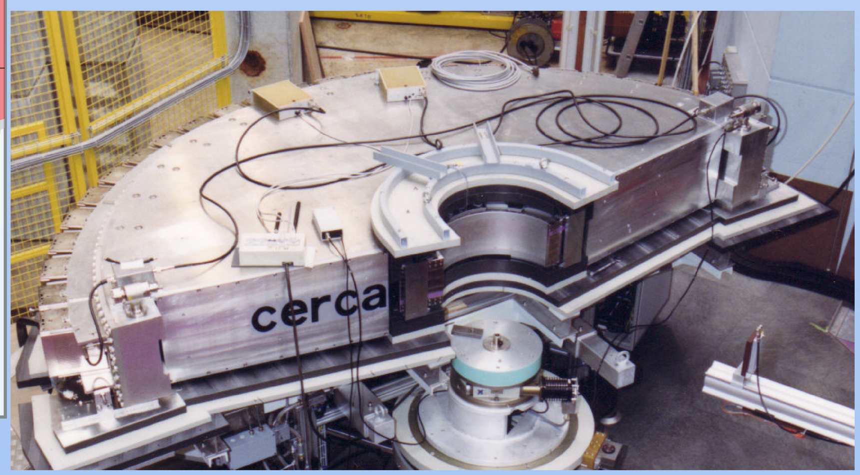

CERCA LCP1600 detector

- 1600 wires with angular separation 0.1° (2.6mm)
- ^{3}He (3.6 bar) + CF_4 (1.1 bar), effective detection length 3.5 cm
- Efficiency 80% @ 1.5 Å
- Gas mixture cleaning/pressurising system

Pulse height spectrum PHS

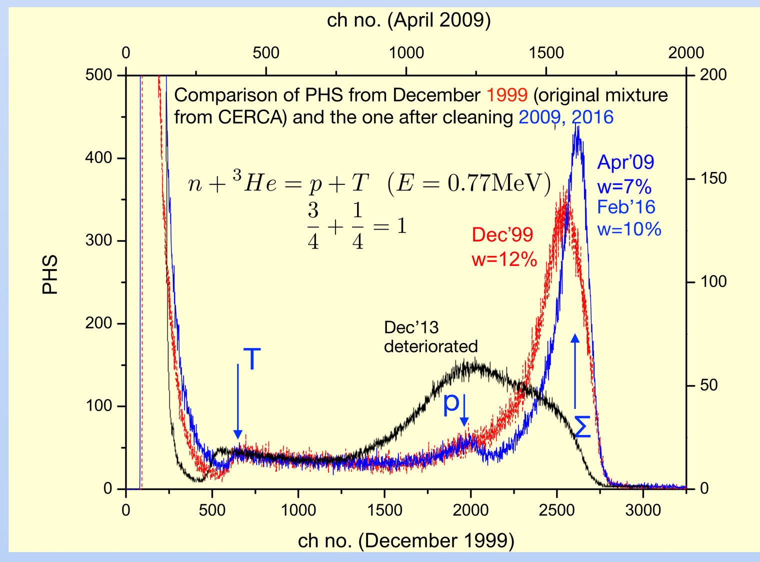

HRPT features

- Neutron wavelengths (0.94-2.96) Å
- Range of 2θ=0-165° → high Q ≤ 13 Å^{-1}
- High resolution δd/d =10^{-3}
- 1600- ^{3}He detectors with angular separation 0.1°
- Vertically focusing wafer Ge(*hkk*)monochromator 28.5cm high, total mosaic halfwidth 15'
- Flexible resolution/intensity:
  - primary beam collimations 6', 12', 24'
  - slit system for secondary collimation <40'
  - monochromator take-off-angle 90° and 120°
- Oscillating mylar-GdO_3 radial collimators to eliminate Bragg peaks from sample environment (FWHM 14 mm and 7 mm) e.g. cryostat or furnace
- Low background. ≤30 mm³ sample is possible
- Sample environment
  - sample changers for eight (room T) and five (1.5-320K) samples with rotation along z.
  - computer controlled motorised *xy*-sample table and (+/-*yz*) beam reduction
  - zero matrix pressure cells (9 , 15 , 100 kbar)
  - standard LNS sample environment: T=80mK—1800K, H=6T(vertical)
  - automatic He, N2 refilling

Ge monochromator

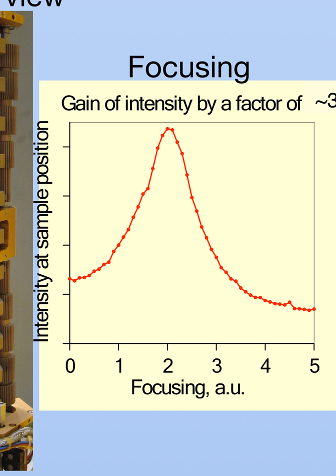

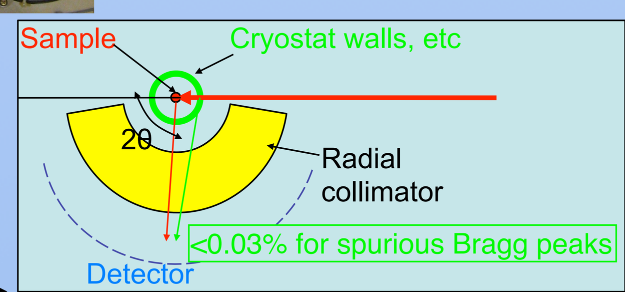

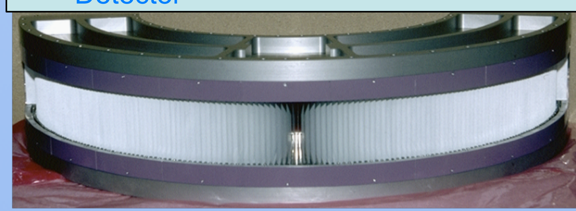

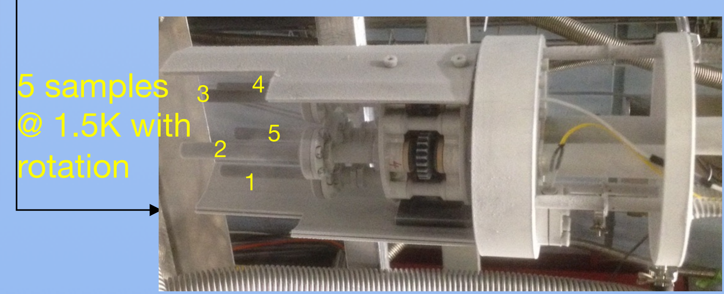

Flexible choice of wavelength, resolution/intensity

- Wavelength is selected by (hkk) plane of Ge-monochromator
- Resolution and intensity are controlled by appropriate primary/secondary collimations and take-off-angle of the monochromator (120° or 90°)

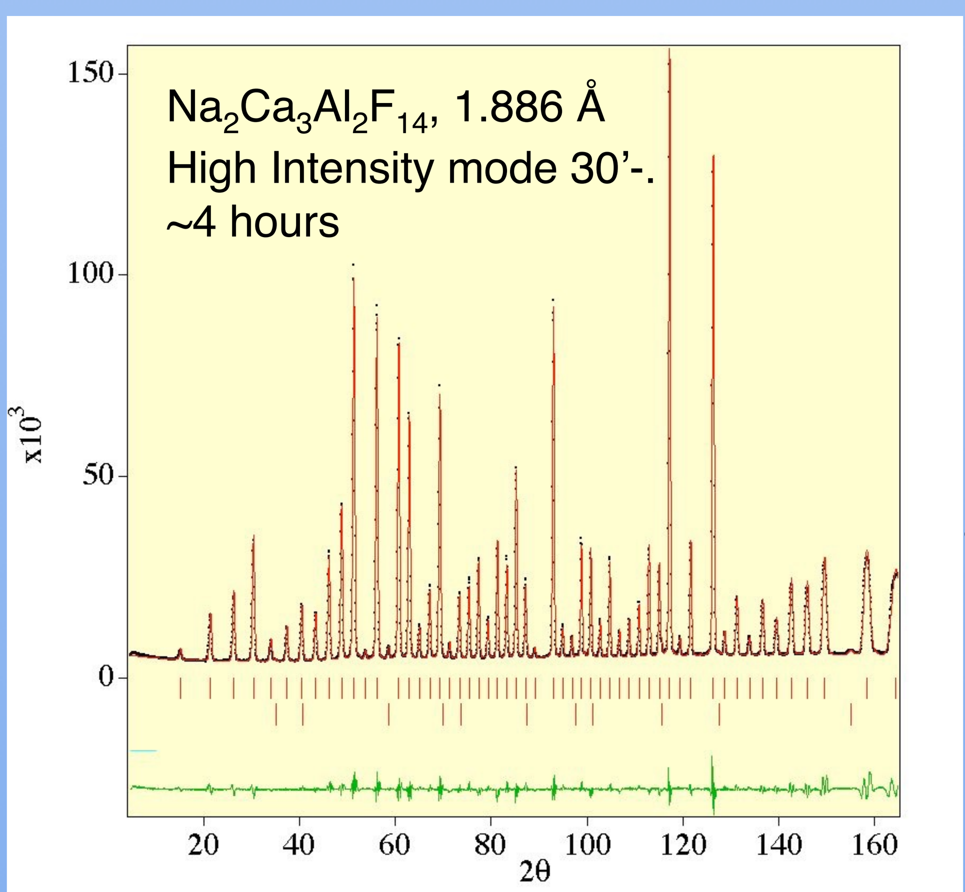

HRPT RESOLUTION FUNCTIONS

(FWHM, 2θ$_M$ = 120°)

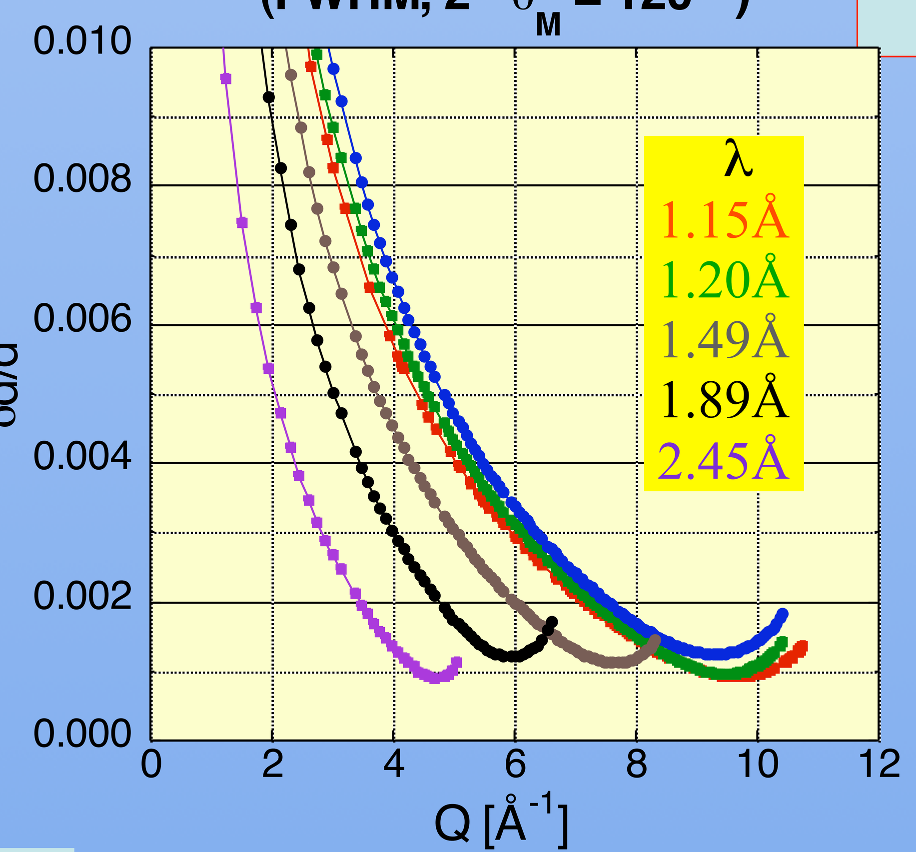

Possible choice of neutron wavelength and corresponding effective counting rates (calib. by V) of the HRPT detector relative to the choice of λ= 1.886 Å in HI mode without primary collimation (40').

	2θ$_M$=90°		2θ$_M$ = 120°	
(hkk) Ge	λ, Å	Effective intensity	λ, Å	Effective intensity
311	2.40971	0.64	2.9536	~0.16
400	1.9984[4,5]		2.4491[1,3]	0.19
133	1.8324	1	2.2461[1,2]	
511	1.5384	1.55	1.886	1
533	1.2183	0.83	1.494	0.9
711	1.1194	0.6	1.372	0.71
733	0.9763	0.34	1.197	0.63
822	0.9419	0.48	1.154	0.79
466			1.044	0.27

[1]PG(C) filter
[2]1/3 λ contamination
[3](2/3)λ contamination due to double Bragg scattering is avoided by rotating the monochromator along the Q.
[4] 1/2 λ contamination
[5] 2/3 λ contamination
[6] Bragg intensity 45%, long (140mm) PGC filter, 8.8% contamination by λ=2.97 Å (refinable).

Comparison of resolution functions for different primary-secondary collimations. Typical modes are HI:40'-, MR:12'-24', HR:6'-12'. Counting rates are decreased by a factor of ~3 and ~(8-10) for MR and HR, respectively.

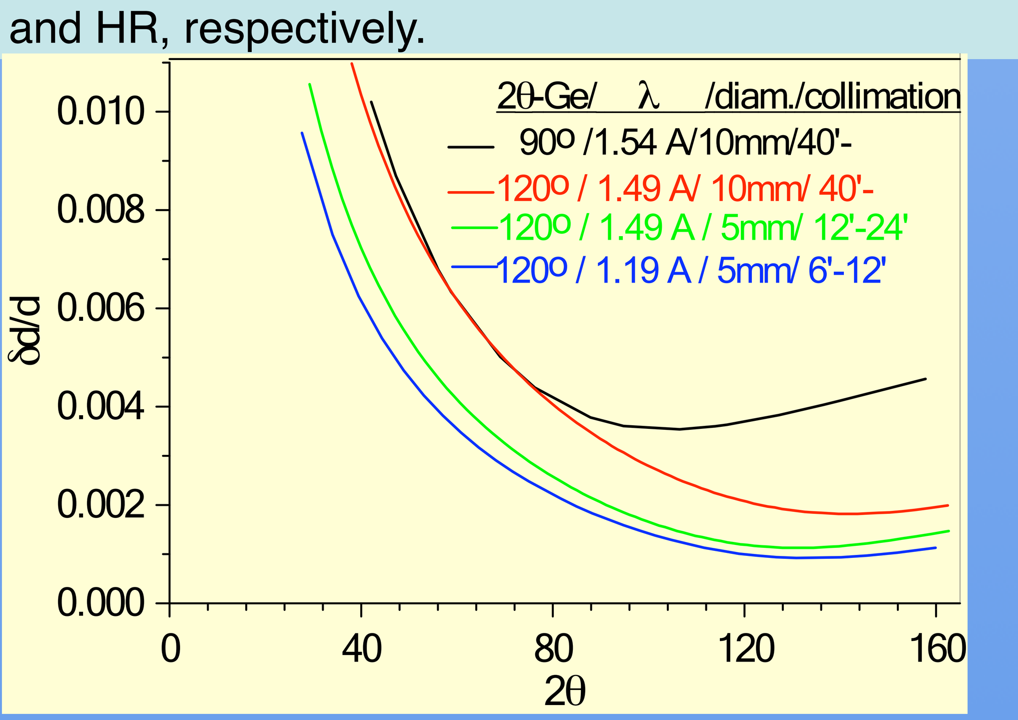

Applications

- Precise structure refinement complementary to X-rays
- Magnetic ordering phenomena
- Detection of lattice distortions, defects, internal strains from (anisotropic) line broadening
- Phase analysis of new materials, direct structure solution
- Real time studies of chemical, structural, magnetic changes

Iron vacancy superstructure and room temperature antiferromagnetic order in superconducting $X_yFe_{2-x}Se_2$ (X=K, Cs, Rb)

A unique feature of the new alkali-metal intercalated iron selenides $X_yFe_{2-x}Se_2$ (X = K, Cs, Rb) discovered towards the end of 2010 is the presence of robust antiferromagnetism with an extraordinary high Néel temperature above 500 K, and high-temperature superconductivity with a critical temperature at around 30 K. Another interesting specific feature of this new class of magnetic superconductors is the presence of an iron vacancy superstructure. Concomitantly with the vacancy ordering, the ordering of the rest of the iron atom spins have the same propagation wave vector at almost the same temperature with the iron magnetic moment ranging from 2.1 to 2.6 μ_B at 300K. The presence of such strong magnetism may come as a surprise to superconductivity experts and increases the demand for new ideas to rationalize this phenomenon.

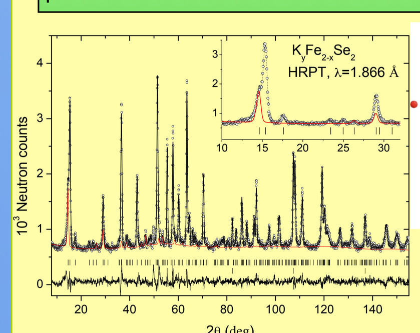

The Rietveld refinement pattern and difference plot of the neutron diffraction data. The magnetic contribution together with the background is shown by a red line.

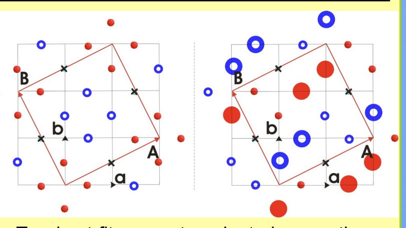

Two best-fit symmetry adapted magnetic configurations in a projection of one layer of Fe on the *ab*-plane. Iron vacancy positions are shown by crosses. Open blue and filled red circles show Fe down and up spins. Large red unit cell (**A,B**) corresponds to the supercell with vacancy ordered structure.

The satellite reflections are indicated by arrows for **k**1 = [2/5 ,1/5 ,1] and **k**2 = [1/5 , 2/5 ,1] by solid and dashed lines These two *k* vectors correspond to two twin domains.

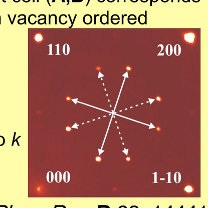

Pomjakushin *et al* 2011 *J. Phys.: Condens. Matter* 23 156003; *Phys. Rev.* **B** 83, 144410

The crystal structures of two polymorphs of the vaterite-type rare earth orthoborates,i.e., the low- and high-temperature modifications of $(Y_{0.92}Er_{0.08})BO_3$, were solved and refined from neutron powder diffraction data.

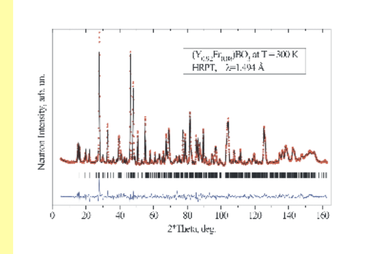

The low-temperature polymorph crystallizes in a C-centered monoclinic cell with $C2/c$ space symmetry, the unit cell parameters being a = 11.3138(3), b = 6.5403(2), c = 9.5499(2) E and β = 112.902(1)°. The boron atoms in the structure are all tetrahedrally coordinated and forming the 3-membered ring borate B_3O_9 groups.

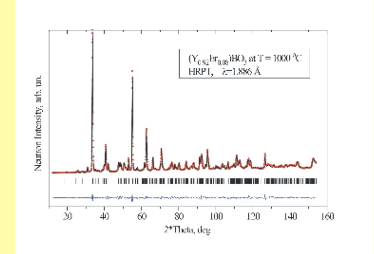

The high-temperature form crystallizes in a new structure type in a monoclinic cell with $C2/c$ space symmetry, and the unit cell constants: a = 12.2019 (3), b = 7.0671 (2), c = 9.3424 (2) E, β = 115.347 (1)°. The borate groups in the high-temperature structure are all isolated flat BO_3 triangles.

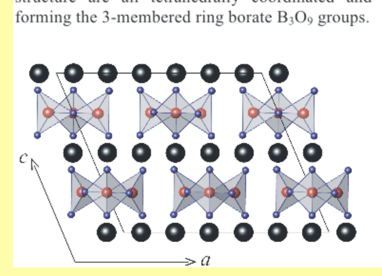

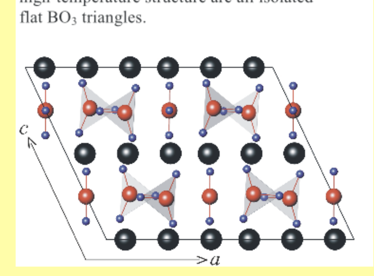

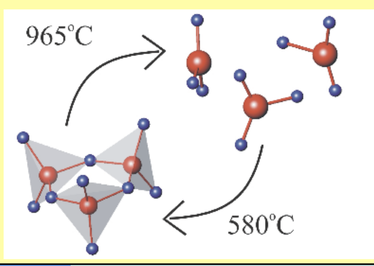

At the phase transition, one B-O bond per each of the BO_4 tetrahedra in the B_3O_9 ring borate group, is broken, thus leading to the purely triangular BO_3 borate groups at high temperature.

Details of this study may be found in:
J. Lin, D. Sheptyakov, Y. Wang and P. Allenspach, *Chem. Mater.* **16**, 2418-2424 (2004).

Reference

[1] **P.Fischer**, G. Frey, M. Koch, M. Koennecke, V. Pomjakushin, J.Schefer, R. Thut, N. Schlumpf, R. Buerge, U. Greuter, S. Bondt, and E. Berruyer *"High-resolution powder diffractometer HRPT for thermal neutrons at SINQ"*, Physica B **276-278**, 146-147 (2000).